

Towards High-Resolution functional Ultrasound (fUS) Imaging of the Murine Spinal Cord

S. Soloukey^{a,b}, B.S. Harhangi^b, B.S. Generowicz^a, J.P.H. Slenter^a, C.I. De Zeeuw^{a,c}, P. Kruizinga^{a,d}, S.K.E. Koekkoek^a

^a Department of Neuroscience, Erasmus MC, Rotterdam, The Netherlands

^b Department of Neurosurgery, Erasmus MC, Rotterdam, The Netherlands

^c Netherlands Institute of Neuroscience (NIN), Royal Dutch Academy for Arts and Sciences, Amsterdam, The Netherlands

^d Department of Biomedical Engineering – Thorax Center, Erasmus MC, Rotterdam, The Netherlands

s.soloukey@erasmusmc.nl, b.s.harhangi@erasmusmc.nl, b.generowicz@erasmusmc.nl, j.slenter@erasmusmc.nl, c.dezeeuw@erasmusmc.nl, p.kruizinga@erasmusmc.nl, s.koekkoek@erasmusmc.nl

Abstract—While functional Ultrasound (fUS) is taking flight as a new high-resolution imaging tool for the brain, its application for spinal cord imaging has been mostly neglected so far. This, while the spinal cord plays an essential role in some of the questions currently asked in neuroscience. The current paper is the first to attempt to apply fUS to the mouse spinal cord, using an electrical epidural stimulation paradigm relevant to the current clinical questions being asked in e.g. the realm of spinal cord injury. We demonstrate the power of high-resolution vascular imaging of the murine spinal cord using both 2D and 3D-images and discuss potential applications of this newly available and unprecedented level of detailed microvascular information. In addition, we discuss one of the major problems facing the success of fUS-imaging for the (murine) spinal cord in particular: motion artefacts due to physiological and stimulation-evoked changes in breathing. Lastly, we discuss our vision on the necessary future steps which can facilitate successful fUS-imaging of the murine spinal cord.

Keywords—spinal cord, functional ultrasound, fUS, high-resolution ultrasound, high-frequency, vascular imaging, μ Doppler, epidural electrical stimulation, EES

I. INTRODUCTION

The spinal cord is often considered to be the ‘extension’ of the brain, playing a key role in the physiological exchange of information between the central and peripheral nervous system. The spinal cord also plays a central role in pathologies such as spinal cord injury (SCI), multiple sclerosis and chronic pain. Interestingly, however, during the development of cutting-edge techniques available to the neurosciences, the spinal cord notoriously lags behind the brain in the actual application of these techniques.

This is especially the case for the revolutionary technique of functional Ultrasound (fUS), which has been around for little over a decade [1]. Using the increasingly popular technique of high frame-rate ultrasound imaging, fUS enables the neuroscientist to image in unprecedented detail changes in blood dynamics by visualizing the small-scale motions induced by changes in blood flow, blood volume and vessel diameter. These local changes in blood dynamics may in turn reflect changes in

metabolic activity due to neuronal activity through the process of NVC. Many other neuroimaging techniques, such as fMRI, are also NVC-based [2]. In these imaging techniques, the ‘functional’ information is often obtained by seeking a shared response across multiple pixels or by correlating a pre-determined stimulus pattern with every pixel over time [3].

So far, most fUS-related work has centered around brain-imaging in a range of subjects, including rats [4], birds [5] and primates [6], proving to be a powerful tool for studying the dynamics of endogenous brain signals. The application in spinal cord, however, has remained limited to one feasibility study in swine and rats [7]. However, not only the translation of fUS to the spinal cord itself, but especially the translation of fUS to the mouse spinal cord (the preferred animal of choice in a scale of neuroscientific experiments), is a challenge. Not only in terms of scaling up the frequency of the ultrasound in order to recover the smaller vasculature of the mouse spinal cord, but also scaling up the temporal frequency as the Doppler shifts are inversely proportional to the spatial resolution and the potential faster vascular dynamics involved with the smaller mouse spinal cord as compared to rats. Additionally, with the location of the spinal cord in close proximity to the lungs and the evocation of motion being inherent to the functionality of the spinal cord, motion correction becomes a necessary endeavor. In the current paper we discuss our first steps towards development of fUS-imaging in the mouse spinal cord.

II. MATERIALS AND METHODS

A. Animal Models and Surgical Procedures

A total of n=6 adult, anesthetized C57BL/6 mice (Charles River, NL) were used in the experiments as presented here. Two types of animal models were used in this study for demonstrative purposes: 1) Acute Spinal and 2) Chronic Spinal Experiments. For the acute experiments, a total of n=4 animals were subjected to a laminectomy over vertebral levels T12-L2, exposing the dorsal aspect of the spinal cord involved in muscle control of the hindlimbs. For stimulation purposes, a pair of multi-stranded PFA-coated stainless steel wires (A-M systems 793200, 36 AWG) was placed over each edge of the spinal cord, serving as a bipolar electrode. A small opening (<0.6mm) was made in the PFA-coating using a scalpel, before fixating the wires over the spinal cord. Measurements were performed while using several

This work was funded by the ‘NWO-Groot’ grant (Grant no. 108845) awarded to CUBE, the Center for Ultrasound Brain-imaging @ Erasmus MC.

fixation methods, including conventional spinal clamps and muscle retractors (Stoelting 51690, mouse spinal adaptor), to improve stability of the field of view during breathing and response due to stimulation.

For the chronic experiments, a similar spinal cord exposure was achieved as described for the acute spinal experiments. However, the surgery was designed as a two-stage surgery, first involving the placement of a so-called spinal cord chamber over the region of interest, fixating the spinal column. This chamber was adapted from a previously described version used for repeated multi-photon imaging [8]. After exposure of the spinal cord through laminectomy, the tissue was covered using a 150 μm thick polymethylpentene (TPXTM) plastic window as reported previously by our group [3]. Repeated measurements could be performed up until 3 months post-surgery in a total of $n=2$ animals, after which the windows started detached due to tissue overgrowth. All measurements were performed under anesthesia for vascular imaging purposes (without electrode placement). However, the spinal cord chambers were robust enough to facilitate fixation in an awake animal running on the treadmill.

B. Electrical Stimulation Paradigm

As a stimulation paradigm, we made use of epidural electrical stimulation (EES), a form of spinal cord stimulation currently used in both experimental and clinical settings for the treatment of both chronic neuropathic pain [9], as well as a means for promotion of motor recovery in SCI [10]. In parallel to the report of Song et al. [7], EES was performed using bilateral electrodes over the T12-L2 vertebral levels, as described above. The stimulation pattern consisted of a total of 120 sec of three alternating block of 5 Hz bipolar stimulation (10 sec) and baseline measurements (30 sec). Stimulation amplitudes ranged between 0.05 mA-0.5 mA, depending on the observed response.

C. Ultrasound Acquisition, Image Formation and Post-processing

For the ultrasound data acquisition, we used an ultrasound research system (Vantage 64-LE, Verasonics Redmond, WA, USA) interfaced with a 64 element, high frequency linear array (L35-16v, 69 μm pitch) driven with a 3 cycle burst at 30 MHz. Two transmit-receive events were needed to address the complete aperture, given the 64 channel acquisition. Using our own CPU/GPU data processing software, we were able to achieve continuous, real-time imaging for a long period of time, including the storage of raw beamformed images. The major processing steps include Fourier domain beamforming, SVD clutter filtering [11] and Power Doppler Image (PDI) formation, real-time display and data storage to a 2 TB PCIe SSD. The maximum achievable temporal resolution could be as high as 0.5 ms, while maintaining real-time display (20 Hz) and continuous, raw frame storage (2 KHz), when using for example 6 compounded angled plane waves and an 8.8 by 8 mm field-of-view. For display purposes we enhanced the vascularity by high pass filtering the PDI, up-sampling by linear interpolation, gamma correction and saturation of the highest values. All the post-processing software and the visualization was done in Matlab 2018b (MathWorks Inc.).

In addition, 3D-volumes of the vasculature were created by stacking multiple adjacent 2D-images in a 3D volume offline. We used Paraview (Kitware Inc.), an open-source software tool, for visualizing the 3D vascular volumes.

D. Displacement Score

To determine the motion component in our measurements, we estimated the displacement field between every image at time t to a reference image at $t+1$ for the full length of a functional recording (120 sec) in both the axis along the transducer (x) and the depth-axis (z) using the *imregdemons* tool in Matlab. Additionally, the absolute mean interframe displacement at 20 Hz was calculated for two recording sequences with ascending as well as descending stimulation intensities for comparison purposes.

III. RESULTS

A. Vascular Imaging

During $n=2$ acute spinal cord experiments, both coronal as well as sagittal images were made of the mouse spinal cord. In both planes, the microvascular anatomy of the spinal cord could be distinguished with a spatial resolution up to 50 μm . In the coronal Power Doppler Images (PDIs), multiple large vessels can be well-identified across sections (**Figure 1**), including the central sulcal artery (CSA) which is known to be a vessel of interest for monitoring the pathological mechanisms involved in SCI [12]. In addition, the microvascular structure in the spinal cord tissue in the coronal plane allows for the distinction between grey and white matter.

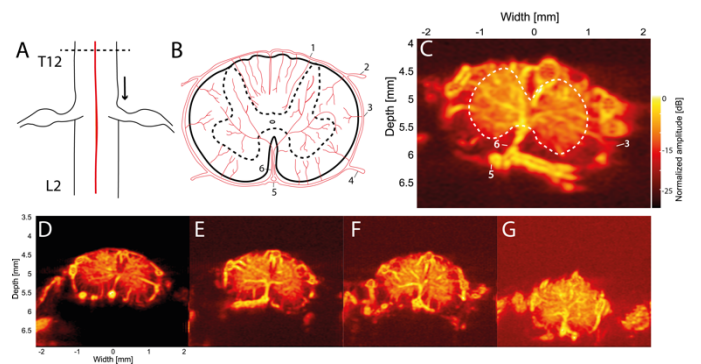


Fig. 1 Overview of the coronal spinal cord images made between vertebral level T12-L2 (A) After exposure of the dorsal aspect of spinal cord using a laminectomy over vertebral levels T12-L2, coronal images were made over the spinal cord in a rostral-caudal direction. (B) Schematic overview of the arterial supply to a coronal section of the spinal cord, as adapted from Mazensky et al. [13]. 1: Dorsal Spinal Artery (DSA); 2: dorsal branch; 3: spinal arterial ring; 4: ventral branch; 5: Ventral Spinal Artery (VSA); 6: central sulcal artery (CSA). Venous complexes are not depicted here. (C) Using fUS, the microvasculature of the spinal cord can be distinguished with a striking resemblance to currently available anatomical schematics based on histopathological work. Interestingly, the rich vasculature of the grey vs. white matter seems to enable a delineation between these two types of tissue on the PDI (white dotted line). (D-G) This series of images provides a sequential overview of the different PDIs as acquired while imaging the spinal cord in the rostral-caudal direction. Due to the natural curvature in the spinal cord, the tissue appears at higher depth as imaging proceeds rostral-caudally. All figures are displayed at a 30 dB dynamic range.

In the sagittal plane, multiple large vessels can also be well-identified in the PDIs (**Figure 2**). The microvasculature reveals the anatomically separated blood supply to the ventral and dorsal aspect of the spinal cord, as well as the pial anastomoses (arterial vasocorona) which encircle the cord and supply the peripheral lateral aspect of the spinal cord.

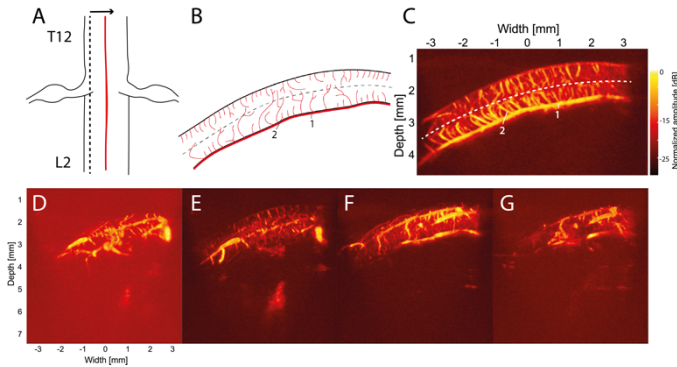


Fig. 2 Overview of the sagittal spinal cord images made between vertebral levels T12-L2 (A) After exposure of the dorsal aspect of spinal cord using a laminectomy over vertebral levels T12-L2, sagittal images were made over the spinal cord in the direction as depicted by the arrow. (B) Schematic overview of the vasculature as seen in a sagittal plain of the spinal cord around the midline. 1: Ventral Spinal Artery (VSA); 2: peripheral branches from the pial plexus. (C) Using fUS, the microvasculature of the spinal cord can be distinguished with a striking resemblance to currently available anatomical schematics based on histopathological work [13]. Interestingly, the PDI clearly shows the differently organized blood-supply for the dorsal (upper) aspect of the spinal cord vs. the ventral (lower aspect) of the spinal cord (white dotted line). (D-G) This series of images provides a sequential overview of the different PDIs as acquired while imaging the spinal cord in from the left to right side. All figures are displayed at a 30 dB dynamic range.

In addition to the 2D PDIs, the acquired sequential images in coronal and sagittal plane were used to make 3D reconstructions by stacking multiple, linearly acquired 2D-images in a 3D volume. In the case of sagittal imaging, this consisted of a total of $n=46$ PDIs, with a $100\ \mu\text{m}$ separation in between (**Figure 3A,B**). In the case of the coronal images, we acquired $n=58$ PDIs, separated by $200\ \mu\text{m}$ each (**Figure 3C**).

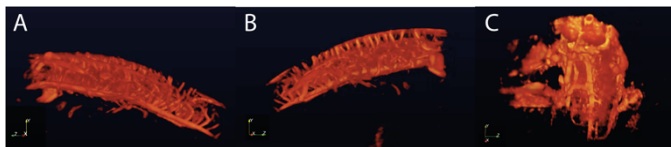


Fig. 3 3D-volume stack of the spinal cord between vertebral level T12-L2. (A) By stacking a total of $n=46$ sagittal PDIs in a 3D-volume, the following 3D-volume stack could be created, revealing the major vascular characteristics of the spinal cord. (B) The same 3D-volume stack but using opposite angle of view as compared to (A). (C) 3D-volume stack created by stacking a total of $n=58$ coronal PDIs in a 3D-volume. The reconstruction is depicted from a slightly tilted angle, to reveal the ventral aspect of the vasculature.

B. Chronic Vascular Imaging

In those animals subjected to a chronic spinal cord chamber, repeated vascular measurements were performed. In **Figure 4** the results of week 1 vs. week 4 of imaging over the TPX-window are depicted, showing little difference in image quality. The spinal cord chamber was stable for up to 3 months (including during awake spinal fixation).

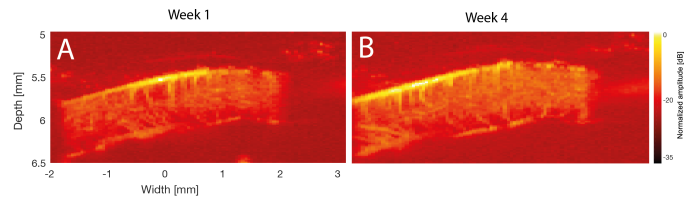


Fig. 4 Overview of spinal cord images under a chronic TPX-window week 1 (left) and week 4 (right) post-implantation. Both images depict a sagittal section of the spinal cord under a TPX window. The shapes on either side of the sagittal plane are the edges of the spinal cord chamber. All figures are displayed at a 30 dB dynamic range.

C. Towards fUS-imaging - Displacement Scoring

To objectively assess the component of motion during EES stimulation trials, the displacement during functional recordings was determined. In one of the animals subjected to functional imaging, a sequential set of trials under different stimulation intensities (in ascending as well as descending order) was recorded. As depicted in **Figure 5**, the mean absolute interframe displacement of each trial was higher under higher stimulation intensities, objectifying the empirically observed response of the animals to the EES, both in terms of hindlimb muscle response as well as breathing.

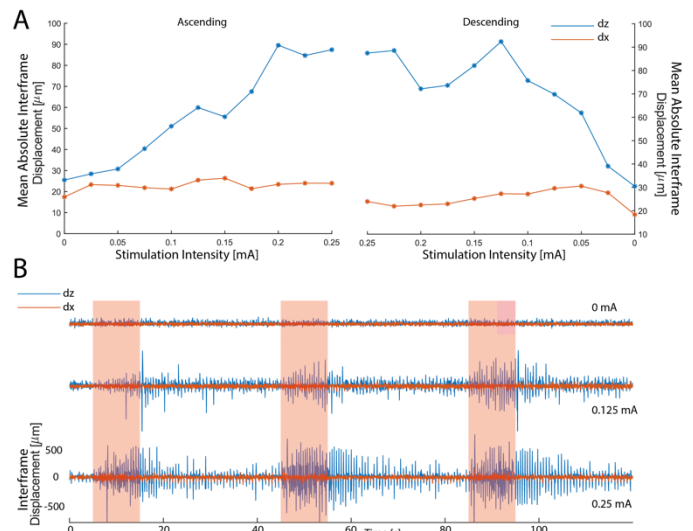


Fig. 5 Overview of results of interframe displacement calculations for a series of sequential measurements under ascending and descending stimulation intensities. (A) Overview of the mean absolute interframe displacement at 20 Hz in both the x - and z -axis during an ascending (left) and descending (right) sequence in stimulation intensities. As becomes clear, the biggest component of movement is found in the z -axis. This is to be expected, based on the direction of movement of the spinal cord during breathing. Interestingly, as the stimulation intensity rises, the displacement increases as well, which is to be expected. However, this relative rise during increase in stimulation intensity is different for the ascending vs. descending sequence, indicating an after-effect of exposure to previous stimulation intensities, which is relevant to take into consideration during experimental designs and post-processing. (B) Three examples traces at three different stimulation intensities (0 mA, 0.125 mA and 0.25 mA), showing the displacement over time during the duration of a single functional recording. During the stimulation blocks (red squares), relative displacement seems to increase, with an after-effect in the post-stimulus blocks. This displacement is higher in the 0.25 mA trial as compared to the 0.125 mA trial, as is to be expected based on the results in (A). x -axis= along the transducer (left and right), z -axis= depth-axis (up and down).

IV. DISCUSSION

The current paper demonstrates the potential power of using fUS in the murine spinal cord. In terms of vasculature, the unprecedented spatiotemporal resolution in combination with the chronic animal models described above, allows for long-term monitoring of microvascular, anatomical changes. The need for this combination of benefits in one single technique exists for a scala of biological questions. In SCI, for instance, high-resolution monitoring of vascular events is important as promotion of neovascularization after injury has the potential to improve neuronal regeneration and long-term functional recovery. In a neurosurgical setting, vascular monitoring with this level of detail can be of great value for spinal cord tumor monitoring or intra-operative tumor delineation. Improved understanding of the vascular 3D morphological changes involved in disease development can provide crucial insight into the relationship of these changes with the pathology, and thus may allow development of novel and effective therapeutic strategies to improve long-term outcomes for patients.

In terms of functionality, the possibility to reach high-resolution functional imaging in the spinal cord using fUS can be revolutionary, both in terms of understanding endogenous signals in the spinal cord, as well as understanding and developing techniques for the clinic, such as EES as used in the current study. However, the current paper also demonstrates the inherent difficulty of using an imaging technique that relies on blood motion as the main source of contrast in a motion-evoking stimulation paradigm. In our data so far, we have not been able to convincingly conclude the presence of functional signal as a response to EES stimulation. Even though the correlation plots presented might suggest otherwise. (*Data not shown here*), the motion artefacts in our dataset so far, do not exclude the possibility of artefactual correlation values. The fact that the increase in motion during our functional measurements is a response to the stimulation itself, complicates the process of motion correction *without* losing the information of interest. Additionally, we found that the induced motion contains a large out-of-plane component for which we cannot correct. A clear solution to this problem would be full-fledged 3D fUS.

The other possibilities for improvement of the particular set of challenges posed by motion lie in both the technical as well as the neuroscientific domain. First of all, (re)inventing clever fixation methods for spinal cord imaging should further improve stabilization during functional EES trials. Using ventilated animals, allows for further manipulation of the physiological and EES-evoked changes in breathing during functional measurements. Although the acute experimental setting will allow for the potentially beneficial manipulations described above, it can be a complicating factor in itself as it inherently requires the use of anesthesia, which is known to directly affect physiological NVC-processes. Therefore, the development of small-scale, light-weight probes for freely walking spinal cord imaging experiments in awake animals, will be of great value to the field. However, the developments

in terms of motion correction in this respect will need to happen in concordance.

Lastly, it is interesting to note that the problem of the spinal cord lagging behind the brain in the application of neuroscientific techniques, might actually work in two ways. In contrast to the brain, which exists of many cortical and subcortical functional areas, with clear anatomical and often vascular borders, the spinal cord is a less compartmentalized organ. Although the crude division between the dorsal and ventral aspect of the cord allows for the distinction between two greatly different types of signal (afferent vs. efferent respectively), the compartmentalization along the rostral-caudal axis is less well-defined. Knowing these inherent difficulties in spinal cord images, the field of fUS-imaging will need to bear in mind the tissue's specific needs in order to harness the techniques full potential.

ACKNOWLEDGMENTS

The authors would like to express great gratitude to Frits Mastik for the 3D-reconstructions depicted in Figure 3. In addition, the authors would like to thank Romy Schilperoort for her assistance during some of the experiments.

REFERENCES

- [1] T. Deffieux, C. Demene, M. Pernot, and M. Tanter, "Functional ultrasound neuroimaging: a review of the preclinical and clinical state of the art," *Current Opinion in Neurobiology*, vol. 50. pp. 128–135, 2018.
- [2] A. Urban *et al.*, "Understanding the neurovascular unit at multiple scales: Advantages and limitations of multi-photon and functional ultrasound imaging," *Advanced Drug Delivery Reviews*. 2017.
- [3] S. K. E. Koekkoek *et al.*, "High Frequency Functional Ultrasound in Mice," in *IEEE International Ultrasonics Symposium, IUS*, 2018.
- [4] E. Tiran *et al.*, "Transcranial Functional Ultrasound Imaging in Freely Moving Awake Mice and Anesthetized Young Rats without Contrast Agent," *Ultrasound Med. Biol.*, 2017.
- [5] R. Rau *et al.*, "3D functional ultrasound imaging of pigeons," *Neuroimage*, 2018.
- [6] A. Dizeux *et al.*, "Functional ultrasound imaging of the brain reveals propagation of task-related brain activity in behaving primates," *Nat. Commun.*, 2019.
- [7] P. Song *et al.*, "Functional Ultrasound Imaging of Spinal Cord Hemodynamic Responses to Epidural Electrical Stimulation: A Feasibility Study," *Front. Neurol.*, vol. 10, p. 279, 2019.
- [8] M. J. Farrar, I. M. Bernstein, D. H. Schlafer, T. A. Cleland, J. R. Fetcho, and C. B. Schaffer, "Chronic in vivo imaging in the mouse spinal cord using an implanted chamber," *Nat. Methods*, 2012.
- [9] R. B. North, D. H. Kidd, M. Zahurak, C. S. James, and D. M. Long, "Spinal cord stimulation for chronic, intractable pain: Experience over two decades," *Neurosurgery*, 1993.
- [10] N. Wenger *et al.*, "Closed-loop neuromodulation of spinal sensorimotor circuits controls refined locomotion after complete spinal cord injury.," *Sci. Transl. Med.*, vol. 6, no. 255, pp. 1–10, 2014.
- [11] B. S. Generowicz *et al.*, "Efficient and Flexible Spatiotemporal Clutter Filtering of High Frame Rate Images Using Subspace Tracking," in *IEEE International Ultrasonics Symposium, IUS*, 2018.
- [12] Y. Cao *et al.*, "Three-dimensional imaging of microvasculature in the rat spinal cord following injury," *Sci. Rep.*, 2015.
- [13] D. Mazensky, S. Flesarova, and I. Sulla, "Arterial Blood Supply to the Spinal Cord in Animal Models of Spinal Cord Injury. A Review," *Anatomical Record*. 2017.